Electronic and magnetic properties of quaternary (Cu,Ni)MnSb alloys

Josef Kudrnovsky, Vaclav Drchal, Frantisek Maca, Ilja Turek

Electronic and magnetic properties of quaternary (Cu,Ni)MnSb alloys

Journal:	*Philosophical Magazine & Philosophical Magazine Letters*
Manuscript ID:	TPHM-08-Apr-0123
Journal Selection:	Philosophical Magazine
Date Submitted by the Author:	01-May-2008
Complete List of Authors:	Kudrnovsky, Josef; Isntitute of Physics AS CR, Theoretical Drchal, Vaclav; Institute of Physics AS CR, Theoretical Maca, Frantisek; Institute of Physics AS CR, Theoretical Turek, Ilja; Institute of Physics of Materials AS CR
Keywords:	density-functional theory, magnetic alloys
Keywords (user supplied):	Curie temperatures, exchange interactions
Note: The following files were submitted by the author for peer review, but cannot be converted to PDF. You must view these files (e.g. movies) online.	
PW_philmag.tex	

RESEARCH ARTICLE

Electronic and magnetic properties of quaternary (Cu,Ni)MnSb alloys

J. Kudrnovský[a], V. Drchal[a], F. Máca[a] and I. Turek[b]

[a] Institute of Physics AS CR, Na Slovance 2, CZ-182 21 Praha 8, Czech Republic
[b] Institute of Physics of Materials AS CR, Žižkova 22, CZ-61662 Brno, Czech Republic

(*Received 00 Month 200x; final version received 00 Month 200x*)

Magnetic properties and Curie temperatures of semi-Heusler alloys $Cu_{1-x}Ni_xMnSb$ are calculated as a function of the alloy composition. The transition from the ferromagnetic state (NiMnSb) to the antiferromagnetic state (CuMnSb) gives rise to an abrupt change in the concentration dependence of alloy magnetization at about $x_{Cu} = 0.7$ while the Curie temperature decreases monotonically with the Cu-content. Such behavior can be understood as due to the onset of disorder in orientations of Mn-spins at $x_{Cu} = 0.7$. A simple account of magnetic disorder as based on the uncompensated disorder local moment picture provides also a good quantitative understanding of available experimental data.

Keywords: density functional theory; exchange interactions; effective Heisenberg model; magnetic disorder; Curie temperatures; quaternary Heusler alloys

1. Introduction

Heusler alloys, both conventional and semi-Heusler ones, represent materials with interesting physical properties. Because of structural similarity with semiconductors and Curie temperatures above the room temperature Heusler alloys are materials interesting for spintronics. This has motivated recent theoretical studies [1, 2] of such compounds while previous experimental studies are reviewed in Ref. [3]. The study of conventional ordered Heusler alloys is now rather common but the situation differs for disordered Heusler alloys. We mention two recent theoretical studies of properties of disordered Heusler alloys over a broad concentration range [4, 5] where the effect of disorder was treated in the framework of the coherent-potential approximation (CPA).

Most of Heusler alloys are ferromagnetic. The system (Cu,Ni)MnSb is therefore of interest as the end-point alloys, NiMnSb and CuMnSb, are ferromagnet and antiferromagnet, respectively. Theoretical and experimental studies of NiMnSb alloys are frequent as contrasted with corresponding studies of CuMnSb alloys. We mention a recent comprehensive theoretical study of electronic properties of CuMnSb [6]. Extensive experimental studies of various properties of (Cu,Ni)MnSb quaternary alloys including measurements of magnetic properties and Curie temperatures were done recently [7, 8]. The main conclusion from experimental studies is a dramatic concentration dependence of magnetization with a pronounced break at about 70% of Cu-content as contrasted with a smooth concentration behavior

e-mail: kudrnov@fzu.cz, drchal@fzu.cz, maca@fzu.cz
e-mail: turek@ipm.cz

ISSN: 1478-6435 print/ISSN 1478-6443 online

DOI: 10.1080/1478643YYxxxxxxxx
http://www.informaworld.com

observed for Curie temperatures. Such behavior can be qualitatively understood as due to the onset of disorder in spin-orientations on structurally perfect Mn-sublattice induced by the disorder of (Cu,Ni)-sublatice. Such disorder will reduce the spin magnetic moment but exchange integrals between large, rigid Mn-moments will be only weakly influenced by the magnetic disorder. Consequently, Curie temperatures can be estimated with a reasonable accuracy from those corresponding to the ferromagnetic state over the whole concentration range without abrupt cocentration change. Varying alloy composition will change the carrier cocentration and corresponding modification of the Fermi-surface topology will influence exchange integrals despite the fact that Mn-sublattice remains structurally perfect. Another consequence of the varying carrier concentration is the modification of energy separation between the system Fermi energy and unoccupied Mn 3*d*-states which gives rise to an increased superexchange interaction and thus influences the values of exchange integrals as demonstrated recently for Heusler alloys with disorder on the *sp*-sublattice [9]. Finally, the rather large Mn-Mn distance in Heusler alloys gives rise to relatively narrow Mn spin-subbands, so that the effect of electron correlations in Mn-subbands may be non-negligible.

We wish to study concentration dependence of magnetic moments and Curie temperatures in semi-Heusler alloys (Cu,Ni)MnSb in the framework of the parameter-free approach based on the density functional formalism. We have also investigated how the results depend on electrons correlations in narrow Mn-subbands. We will describe electron correlations on Mn-atoms in terms of a simple LDA+U approach [10, 11]. Calculated results will be compared with available experimental data.

2. Formalism

All calculations were performed using the tight-binding linear muffin-tin orbital (TB-LMTO) approach and the effect of substitutional Cu-Ni disorder was described by the CPA [12]. We used scalar-relativistic form of the TB-LMTO, *spdf*-basis, the Vosko-Wilk-Nusair exchange-correlation potential, and the same radii for constituent atoms. The lattice constants were taken from the experiment and they obey reasonably well the Vegard's law. The effective Hubbard parameter $U_{\rm eff}$=0.13 Ry which was used in the LDA+U calculations is same as that used in related Heusler alloys [11]. The magnetic disorder was treated in the framework of the uncompensated disordered local moment (uDLM) model: we assume that magnetic disorder (for $x_{\rm Cu} \geq 0.7$) will be characterized by some amount $\mathrm{x}^{-}_{\rm Mn}$ of Mn-spins pointing in the direction opposite to the rest of Mn-spins $\mathrm{x}^{+}_{\rm Mn}$ in such way that the condition $\mathrm{x}^{+}_{\rm Mn}$+$\mathrm{x}^{-}_{\rm Mn}$=1 is fulfilled. In the DLM state it holds $x^{+}_{\rm Mn}$=$x^{-}_{\rm Mn}$=0.5. One can, of course, imagine many possible scenarios for such a complicated transition. We have used the simplest one, i.e., the linear increase of $x^{-}_{\rm Mn}$ with Cu-concentration starting from $x_{\rm Cu} = 0.7$ and with the DLM state for $x_{\rm Cu} = 1$. We have then simply $\mathrm{x}^{-}_{\rm Mn} = (5/3)\,(\mathrm{x}_{\rm Cu} - 0.7)$. The uDLM state can be also described in the framework of the CPA [12].

The thermodynamical properties of the system were described by the classical Heisenberg Hamiltonian [13, 14]

$$H_{\rm eff} = -\sum_{i,j} J_{ij}\, \mathbf{e}_i \cdot \mathbf{e}_j \ , \qquad (1)$$

where i, j denote the site indices, $\mathbf{e}_i$ is the unit vector pointing along the direction of the local magnetic moment at the site i, and J_{ij} is the exchange integral between magnetic atoms at sites i and j. The exchange integrals contain, by construction,

the atom magnetic moments and their positive (negative) values indicate the ferromagnetic (antiferromagnetic) coupling. As explained in the Introduction, the exchange integrals were evaluated by assuming the ferromagnetic (FM) reference state. In this paper we neglect exchange integrals connected with small induced magnetic moments on Ni-sites. We have demonstrated recently [4] that this is a reasonable approximation for NiMnSb Heusler alloys. Although non-negligible in general, such exchange integrals are limited to the first-nearest neighbors with a small coordination of four.

We determine the Curie temperature corresponding to the effective Heisenberg model (1) in the framework of both the mean-field (MFA) and the random-phase (RPA) approximations [15]. The MFA estimate of the Curie temperature is

$$k_B\, T_c^{\mathrm{MFA}} = \frac{2}{3} \sum_{i \neq 0} J_{0i}^{\mathrm{Mn,Mn}}\,, \tag{2}$$

where the sum extends over many nearest-neighbor shells. An improved description of the finite-temperature magnetism is provided by the RPA which is given by

$$(k_B\, T_c^{\mathrm{RPA}})^{-1} = \frac{3}{2} \frac{1}{N} \sum_{\mathbf{q}} [J^{\mathrm{Mn,Mn}}(\mathbf{0}) - J^{\mathrm{Mn,Mn}}(\mathbf{q})]^{-1}\,. \tag{3}$$

Here N denotes the number of $\mathbf{q}$-vectors used in the sum over the Brillouin zone and $J^{\mathrm{Mn,Mn}}(\mathbf{q})$ is the lattice Fourier transform of the real-space exchange integrals $J_{ij}^{\mathrm{Mn,Mn}}$. We have used up to 62 shells in the MFA (3) and in the lattice Fourier transform of $J^{\mathrm{Mn,Mn}}(\mathbf{q})$ in (3) and tested the convergence with respect to the number of shells included in the statistical study. The estimated computational error corresponding to a limited number of shells used in calculations is about ± 5 K. We refer the reader to Refs. [4, 14, 15] for further details.

3. Results and discussion

In this section we presents results for magnetic and thermodynamical properties of (Cu,Ni)MnSb alloys over the broad concentration range. Curie temperatures will be estimated for both the LDA and LDA+U approaches.

3.1. *Electronic and magnetic properties*

We present in Fig. 1 various densities of states (DOS). NiMnSb, ($Cu_{0.5}$ $Ni_{0.5}$)MnSb, and CuMnSb in the FM state are shown in Fig. 1. NiMnSb is the halfmetal (the Fermi energy lies in the gap of the minority states) whilst the (Cu,Ni)MnSb alloy becomes metallic with incresing Cu-content. Two important trends have to be pointed out: (i) with increasing Cu-concentration the Fermi energy moves towards the unoccupied states (dominated by Mn d-states). As a result, the superexchange part of exchange integrals gets larger and this effect gives rise to their strong modification with alloying (see also Sec. 3.2); and (ii) the different positions of Cu- and Ni-local DOS indicate strong substitutional disorder in the energy region (-0.4, -0.15) Ry below the Fermi energy (see Fig. 1b). The disorder thus influences states in the energy region far from the Fermi energy as contrasted with the case of conventional fcc-(Cu,Ni) alloy where the Fermi energy lies in the energy region strongly perturbed by the alloy disorder. It should be noted that Mn-majority

states hybridize strongly with Ni-states (see figure (b) in the frame) while their hybridization with Cu-states is weak. The minority Mn-states only weakly hybridize with both Cu- and Ni-states due to their separation in energy. The effect of electron correlations in narrow Mn-subbands is demonstrated in the middle frame for $(Cu_{0.5}\ Ni_{0.5})MnSb$ alloy.

Figure 1. Total and component (Cu,Ni) resolved densities of states (DOS) for the ferromagnetic (Cu,Ni)MnSb alloys: (a) an ordered NiMnSb, (b) disordered $(Cu_{0.5}\ Ni_{0.5})MnSb$, and (c) an ordered CuMnSb. The Cu(Ni)-component DOSs for NiMnSb (CuMnSb) correspond to single Cu(Ni)-impurity in the NiMnSb (CuMnSb) host crystal.

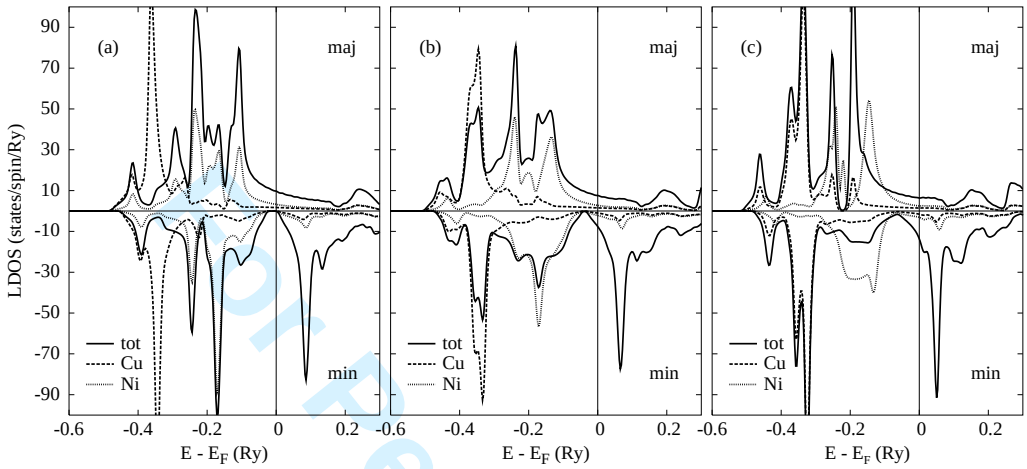

The calculated concentration dependence of magnetic moments is shown in Fig. 2 together with the experimental data [7, 8]. Overall good agreement between theoretical and experimental averaged moments is found over the whole concentration range. It should be noted that the FM calculations fail to reproduce experimental data for $x_{Cu} > 0.7$. This is illustrated by empty circles in Fig. 2. The concentration dependence of local magnetic moments on Mn- and Ni-sites is weak. Both Mn^+ and Mn^- moments have almost the same sizes as expected for well-defined local magnetic moments. The induced moments on the Ni-sublattice are rather small ($m^{Ni} < 0.5\ \mu_B$). We can thus conclude that our simple model of magnetic disorder for Cu-concentrations larger than about 70% explains well experimental data. We have also checked that results for LDA (Fig. 2) and LDA+U (not shown) are similar.

3.2. *Exchange interactions and Curie temperatures*

First five dominating exchange interactions $J_s^{Mn,Mn}$, s=1 to 5, are shown in Fig. 3 as a function of alloy composition. The most remarkable feature is the reduction of the first nearest-neighbor (NN) coupling with increasing Cu-concentration. It is due to the increasing superexchange part of the exchange interaction which originates from the shift of the Fermi energy towards the unoccupied minority Mn-states with Cu-content as discussed above. This interaction is negative and it decreases exponentially with the distance and thus influences mostly the first NN couplings. Other couplings are seen to depend on the concentration only weakly. Dominating but with Cu-concentraton decreasing first NN exchange interactions are also responsible for the monotonic decrease of the calculated Curie temperature (see below). On the other hand, the smaller second NN exchange couplings dominate for high

Figure 2. The averaged and local magnetic moments as a function of composition for (Cu,Ni)MnSb alloys in the present model. Mn^{+} and Mn^{-} denote averaged moments for the majority and minority states and $x_{\mathrm{Cu}} > 0.7$ (open circles). The thick dashed line denotes the experiment [7]. Note that Mn^{-} moments are taken with the opposite sign.

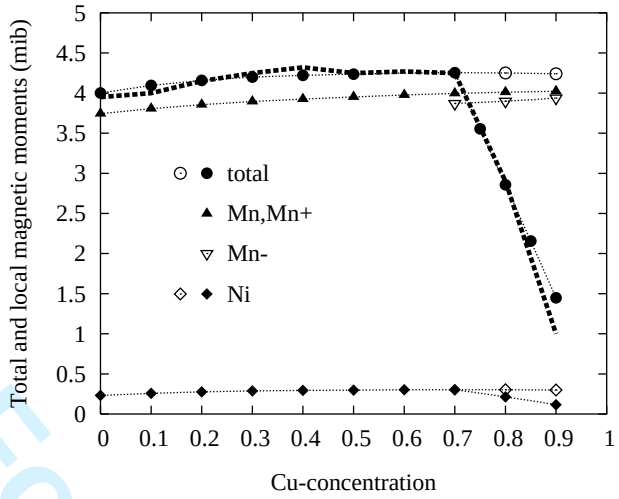

Figure 3. Concentration dependence of the first five dominating (Mn,Mn)-exchange integrals in (Cu,Ni)MnSb Heusler alloys estimated from the ferromagnetic reference state.

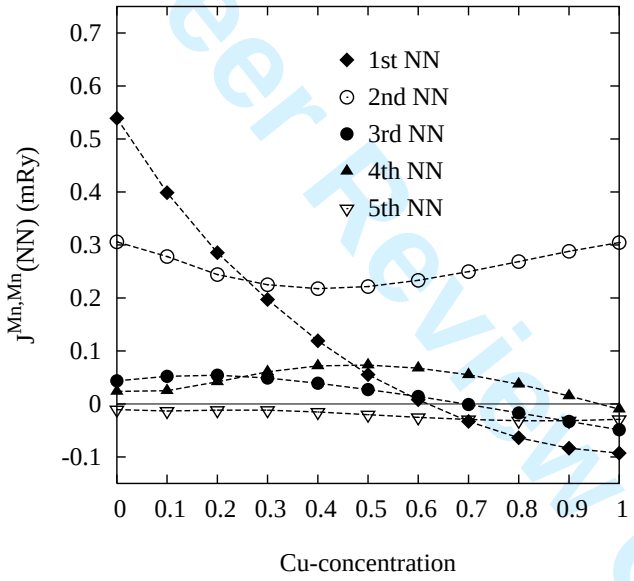

Cu-content. This fact is a precursor of the experimentally observed transition from the FM to the antiferromagnetic (AFM) state of the CuMnSb alloy.

The calculated exchange integrals are used to estimate the Curie temperatures in the framework of both the LDA and LDA+U approximations (see Fig. 4a and 4b, respectively). Both the MFA and RPA estimates of the alloy Curie temperature are shown in Fig. 4 and compared with the experiment. The monotonic decrease of Curie temperatures with increasing Cu-concentration is reproduced by either approximations (MFA and RPA) and in both the LDA and LDA+U methods. The MFA overestimates experimental values as expected while the overall good agreement is found for the RPA. It seems that the LDA+U approach agrees better

with available experimental data, in particular as the shape of the concentration dependence is concerned. The Curie temperature for NiMnSb and the LDA agrees with those obtained in Ref. [4].

Figure 4. Estimated Curie temperatures in the mean-field (MFA) and the random-phase (RPA) approximations: (a) LDA, and (b) LDA+U. The thick dashed lines denote the experiment [7].

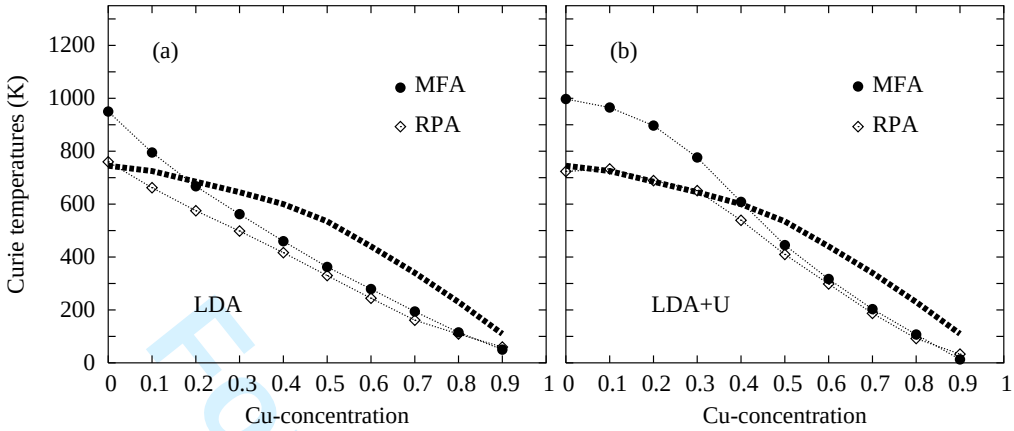

3.3. *Electronic origin of the FM to AFM transition*

The final question we wish to answer here is the origin of the break in magnetization for $x_{\mathrm{Cu}} \approx 0.7$. We have investigated the stability of the FM state with respect to the periodic spin-density fluctuations. The idea is the similar to that used in the alloy

Figure 5. The lattice Fourier transform of (Mn,Mn)-exchange interactions for various Cu-concentrations of (Cu,Ni)MnSb alloy. The maximum indicates the ground state for a given alloy composition.

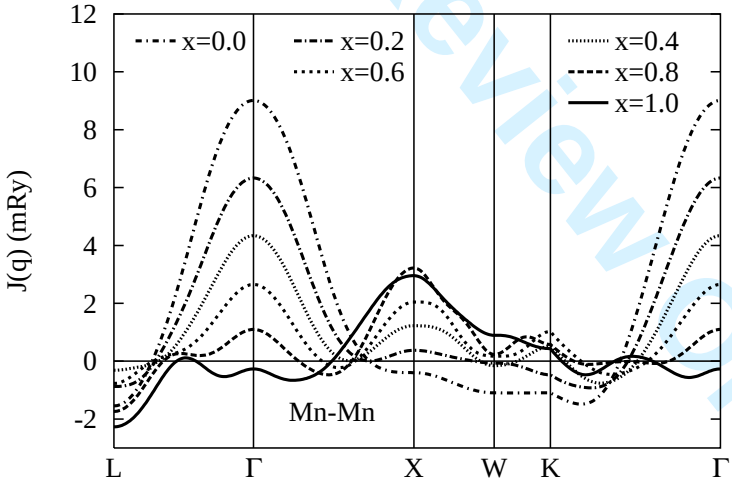

phase stability studies where one investigates the stability of the disordered phase with respect to periodic concentration fluctuations in the framework of the effective Ising model [16]. In the present case we will check the stability of the ferromagnetic phase with respect to the periodic spin fluctuations. One calculates the lattice Fourier transform $J^{\mathrm{Mn,Mn}}(\mathbf{q})$ of real-space exchange integrals $J_s^{\mathrm{Mn,Mn}}$ and searches for its maximum which corresponds to the ground state (see negative sign in Eq. 1).

The concentration dependence of $J^{\mathrm{Mn,Mn}}(\mathbf{q})$ evaluated for the FM reference states is shown in Fig. 5. We observe clearly pronounced maximum for $\mathbf{q} = \mathbf{0}$ for NiMnSb alloy. This means that the energy is minimized by spin-fluctuations with infinitely large wavelengths which, in turn, correspond to the FM ground state. The stability of the FM state, however, decreases with increasing Cu-concentration until for $x_{\mathrm{Cu}} \in (0.6, 0.8)$ we find that a more complex magnetic order becomes energetically favourable. One can identify this fact with the onset of the magnetic disorder on the Mn-sublattice at about 70% of Cu.

4. Conclusions

We have presented parameter-free evaluation of magnetic moments and Curie temperatures of quasi-ternary semi-Heusler (Cu,Ni)MnSb alloy over a broad range of Cu-concentrations which is based on the density functional approach. Using a simple model for a gradual tansition between the ferromagnetic NiMnSb and the antiferromagnetic CuMnSb end-point alloys we have reproduced a pronounced break in the concentration dependence of the averaged magnetic moments found experimentally. We have shown that this transition has a precursor in the ferromagnetic state: the transition is caused by increasing superexchange part of the dominating first nearest-neighbor Mn-Mn interactions which is due to gradual movement of the Fermi energy towards unoccupied Mn-minority subband with increasing Cu-content. Calculated Curie temperatures decrease monotonically with increasing Cu-concentration in agreement with experiment. The RPA-estimates of the Curie temperatures agree reasonably well with experimental data over the whole concetration range.

Acknowledgments

The research was carried out within the projects AVOZ 10100520 and AVOZ 20410507 of the Academy of Sciences of the Czech Republic. Authors acknowledge the financial support from the Grant Agency of the Academy Sciences of the Czech Republic (A100100616), the Czech Science Foundation (202/07/0456), and COST P19 (OC150).

References

[1] I. Galanakis, P.H. Dederichs, and N. Papanikolaou, Phys. Rev. B **66**, 174429 (2002).
[2] E. Sasioglu, L. M. Sandratskii, and P. Bruno, Phys. Rev. B **70**, 024427 (2004)
[3] P.J. Webster and K.R.A. Ziebeck, in *Alloys and Compounds of d-Elements with Main Group Elements, Part 2*, Landolt-Börnstein, New Series, Group III, vol. 19c, ed. by H.R.J. Wijn (springer, Berlin 1988).
[4] J. Rusz, L. Bergqvist, J. Kudrnovský, and I. Turek, Phys. Rev. B **73**, 214412 (2006).
[5] I. Galanakis, E. Sasioglu, and K. Ozdogan, arXiv: 0801.1968 v1.
[6] T. Jeong, R. Wehl, and W.E. Pickett, Phys. Rev. B **71**, 184103 (2005).
[7] S.K. Ren, Y.X. Wang, Y.J. Zhang, G.B. Ji, F.M. Zhang, and Y.W.Du, J. All. Compd. **387**, 32 (2005).
[8] S.K. Ren, W.Q. Zou, J. Gao, X.L. Liang, F.M. Zhang, and Y.W.Du, J. Magn. Magn. Mater. **288**, 276 (2005).
[9] E. Sasioglu, L. M. Sandratskii, and P. Bruno, Appl. Phys. Lett. **89**, 222058 (2006).
[10] A. Shick, V. Drchal, and J. Kudrnovský, Phys. Rev. B **69**, 125207 (2004).
[11] B. Balke, G.H. Fecher, H.C. Kandpal, C. Felser, K. Kobayashi, E. Ikenaga, J.-J. Kim, and S. Ueda, Phys. Rev. B **74**, 104405 (2006).
[12] I. Turek, V. Drchal, J. Kudrnovský, M. Šob, and P. Weinberger, *Electronic Structure of Disordered Alloys, Surfaces and Interfaces* (Kluwer, Boston, 1997); I. Turek, J. Kudrnovský and V. Drchal, in *Electronic Structure and Physical Properties of Solids*, edited by H. Dreyssé , Lecture Notes in Physics, Vol. **535** (Springer, Berlin, 2000), p. 349.

[13] A.I. Liechtenstein, M.I. Katsnelson, V.P. Antropov, and V.A. Gubanov, J. Magn. Magn. Mater. **67**, 65 (1987).
[14] I. Turek, J. Kudrnovský, V. Drchal, and P. Bruno, Philos. Mag. **86**, 1713 (2006).
[15] M. Pajda, J. Kudrnovský, I. Turek, V. Drchal, and P. Bruno, Phys. Rev. B **64**, 174402 (2001).
[16] F. Ducastelle, *Order and Phase Stability in Alloys* (North-Holland, Amsterdam, 1993).

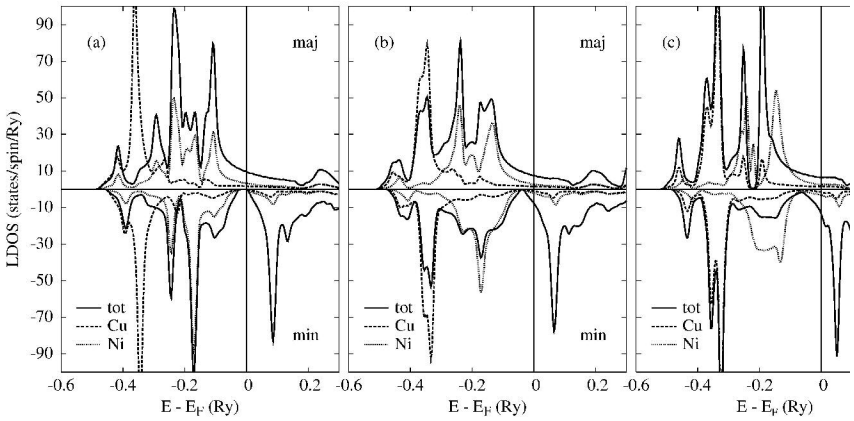

215x279mm (600 x 600 DPI)

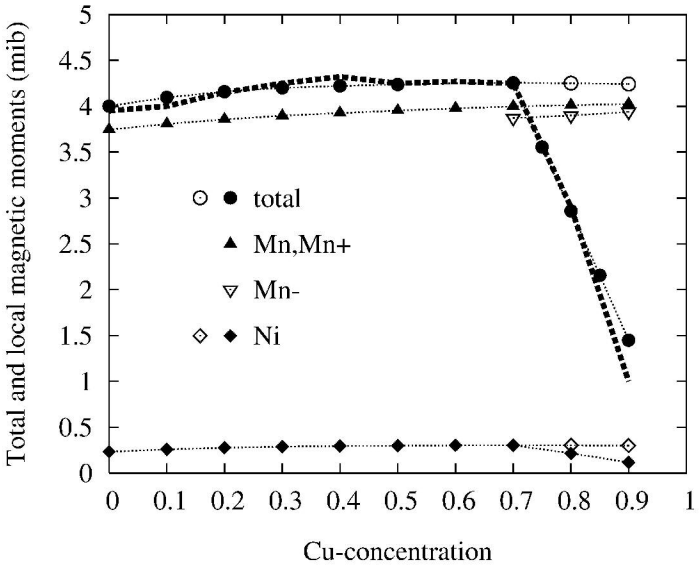

215x279mm (600 x 600 DPI)

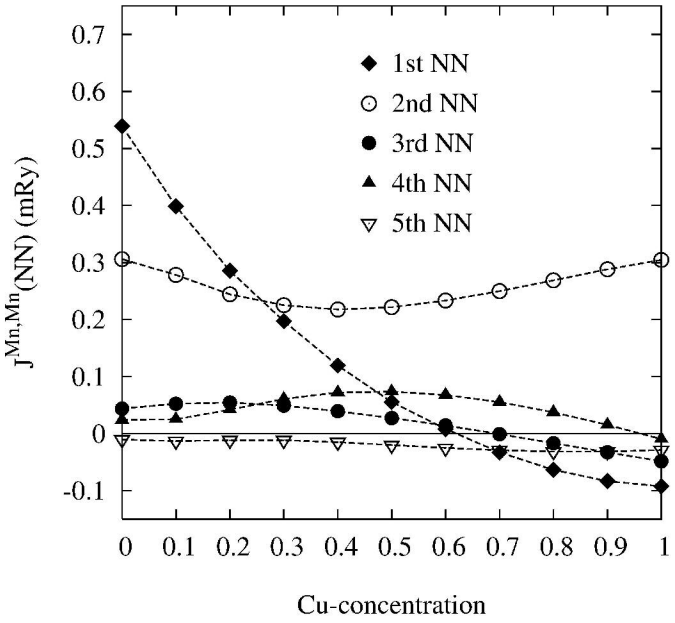

215x279mm (600 x 600 DPI)

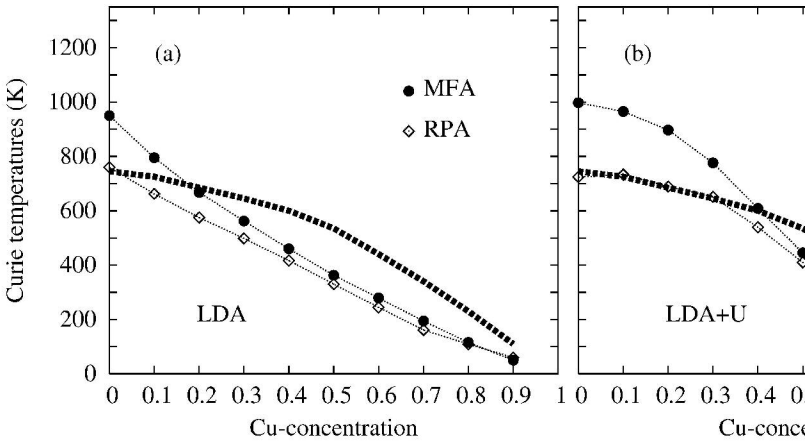

215x279mm (600 x 600 DPI)

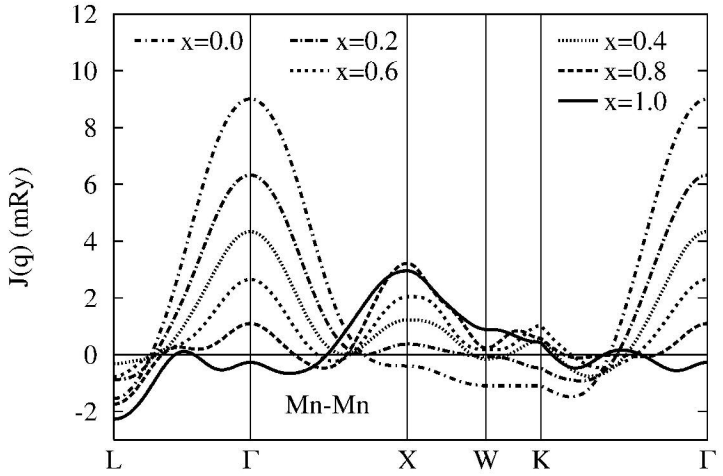

215x279mm (600 x 600 DPI)